2mil

NASA TECHNICAL NOTE

NASA TN D-7707

NASA TN D-7707

SIMILARITY CONSTRAINTS IN TESTING OF COOLED ENGINE PARTS

by Raymond S. Colladay and Francis S. Stepka

Lewis Research Center
Cleveland, Ohio 44135

NATIONAL AERONAUTICS AND SPACE ADMINISTRATION • WASHINGTON, D. C. • JUNE 1974

1. Report No.	2. Government Accession No.	3. Recipient's Catalog No.
NASA TN D-7707		

4. Title and Subtitle	5. Report Date
SIMILARITY CONSTRAINTS IN TESTING OF COOLED ENGINE PARTS	June 1974
	6. Performing Organization Code

7. Author(s)	8. Performing Organization Report No.
Raymond S. Colladay and Francis S. Stepka	E-7376
	10. Work Unit No. 501-24

9. Performing Organization Name and Address	11. Contract or Grant No.
Lewis Research Center National Aeronautics and Space Administration Cleveland, Ohio 44135	

12. Sponsoring Agency Name and Address	13. Type of Report and Period Covered
National Aeronautics and Space Administration Washington, D.C. 20546	Technical Note
	14. Sponsoring Agency Code

15. Supplementary Notes

16. Abstract

A study is made of the effect of testing cooled parts of current and advanced gas turbine engines at the reduced temperature and pressure conditions which maintain similarity with the engine environment. Some of the problems facing the experimentalist in evaluating heat transfer and aerodynamic performance when hardware is tested at conditions other than the actual engine environment are considered. Low temperature and pressure test environments can simulate the performance of actual size prototype engine hardware within the tolerance of experimental accuracy if appropriate similarity conditions are satisfied. Failure to adhere to these similarity constraints because of test facility limitations or other reasons, can result in a number of serious errors in projecting the performance of test hardware to engine conditions.

17. Key Words (Suggested by Author(s))		18. Distribution Statement
Similarity	Test	Unclassified - Unlimited
Heat transfer	Experimental	Category 33
Engine		

19. Security Classif. (of this report)	20. Security Classif. (of this page)	21. No. of Pages	22. Price*
Unclassified	Unclassified	23	$3.00

* For sale by the National Technical Information Service, Springfield, Virginia 22151

SIMILARITY CONSTRAINTS IN TESTING OF COOLED ENGINE PARTS

by Raymond S. Colladay and Francis S. Stepka

Lewis Research Center

SUMMARY

A study is made of the effect of testing cooled parts of current and advanced gas turbine engines at the reduced temperature and pressure conditions which maintain similarity with the engine environment. Some of the problems facing the experimentalist in evaluating heat transfer and aerodynamic performance when hardware is tested at conditions other than the actual engine environment are considered. Low temperature and pressure test environments can simulate the performance of actual size prototype engine hardware within the tolerance of experimental accuracy if appropriate similarity conditions are satisfied. Failure to adhere to these similarity constraints because of test facility limitations or other reasons, can result in a number of serious errors in projecting the performance of test hardware to engine conditions.

INTRODUCTION

A study was made of the operational environments to which cooled parts of advanced engines would be subject and the associated problems that may face the experimentalist in studying or evaluating the performance of these parts. Generally, initial tests of cooled engine parts are conducted with actual prototype hardware but at other than the actual engine gas conditions. This is often the only thing that can be done since available test facilities generally are of lower pressure and temperature than the actual application. In other testing, such as at universities where basic studies of cooling methods are conducted, large scale models of cooled hardware are often used and the gas environment is essentially atmospheric pressure and room temperature. In testing at other than actual engine conditions, a proper understanding of the test-to-engine similarity relations is necessary to assure a meaningful test program.

The purpose of this report is to examine the various similarity parameters that are thought to be important in effecting flow and heat transfer to cooled engine parts and to determine the extent to which these parameters can be maintained at various test and

engine environments. Although the analysis was directed to one of the more critical parts of the engine - the turbine blades - the observations made are applicable to the other cooled engine parts as well. The actual conditions considered in the study were those expected in engines of various types of current and advanced aircraft.

SYMBOLS

d	film injection hole diameter
H	total enthalpy
h	heat transfer coefficient
k	thermal conductivity
L	wall thickness
Nu	Nusselt number
P	total pressure
Pr	Prandtl number
p	static pressure
q	heat flux
R	gas constant
Re_θ	momentum thickness Reynolds number
r	gas constant ratio
St	Stanton number
T	total absolute temperature
t	static absolute temperature
u	velocity
W	mass flow rate
Γ	specific heat function
γ	specific heat ratio
θ	boundary layer momentum thickness
μ	viscosity
ρ	density
φ	dimensionless wall temperature

Subscripts:

aw adiabatic wall with or without film cooling

c coolant

ci local coolant supply

co coolant at film injection location

cr critical condition at Mach number equal to one

g hot gas

ge effective hot gas condition (or recovery condition)

o reference condition

wo hot gas side surface

Superscripts:

(e) engine condition

(t) test condition

ENGINE GAS ENVIRONMENTS

The gas environment properties of initial and primary interest to the experimentalist are the absolute pressures and temperatures since these will dictate whether available test facilities can duplicate or simulate the actual environments. In order to provide a basis on which to analyze constraints that one encounters when attempting to simulate the environments of cooled turbine parts, the range of the expected levels of gas pressures and temperatures of representative future engines are considered. Although the combustion gas environment changes considerably in a given engine depending on the type of aircraft in which it is used and the flight envelope of the aircraft, the operating conditions most applicable to the study herein were thought to be takeoff and cruise. The first is important because it is the condition where the high absolute gas pressures occur and where the short cyclic changes in the environment influence the thermal fatigue life of the hot parts, particularly the turbine. The second condition is where the combustion gas pressures are relatively low because of high cruise altitudes. It is at this operating condition that the hot parts often spend most of their time and which determines their creep and rupture lives.

A tabulation of absolute combustor exit pressures and temperatures and overall compressor pressure ratios at takeoff and cruise conditions for a representative group of engines for four types of advanced aircraft is shown in table I. The first of these

aircraft is a probable next generation of conventional takeoff and landing (CTOL) airplane known as the advanced technology transport (ATT). This aircraft utilizes the supercritical wing (ref. 1) which permits it to cruise at higher speeds than current transports. The engines for this type of aircraft will be high overall pressure ratio, high bypass ratio, turbofans. The second aircraft in table I is the vertical takeoff and landing (VTOL) vehicle which is intended to improve short haul intercity air transportation. The engines for this type of aircraft are generally of moderate overall pressure ratio, high bypass ratio turbo(lift) fans. The third type of aircraft, the short takeoff and landing (STOL) craft, is intended to fill the gap between the CTOL and VTOL by providing service to communities with short runways and between communities separated by greater distances than those served by VTOL and less than those served by CTOL aircraft. The engines for the STOL aircraft are expected to be moderate overall pressure ratio, high bypass turbofans. The last type of aircraft considered is an advanced version of a supersonic (Mach 2.7) transport. This aircraft is intended to provide rapid transportation between distant cities, particularly intercontinental ones. Both turbojet and turbofan engines are being considered for this type of aircraft; the choice is dependent on noise level restrictions. The turbojet would have the lower direct operating cost (DOC) if noise restrictions were not imposed but the duct-burning turbofan would have the lower DOC with noise restrictions imposed. The latter engine is the type considered in table I. It has both a moderately low overall pressure ratio and bypass ratio. The data in table I were obtained from reference 2 or the extrapolation of these data. The table shows several different engine combustion gas environments for the ATT. Each of the engines, with increasing severity of combustion gas environment, is an optimized engine for assumed improvements in turbine cooling and noise reduction technology and capability. Although military aircraft such as supersonic bombers, lightweight fighters, and superiority fighters are not included in the table, their levels of combustion gas environment lie within the range covered by the table. As a result, the observations made herein relative to the testing of hot parts of the commercial engine listed in table I would also be applicable to military engines.

SIMILARITY PARAMETERS

In many instances, the performance of turbine components is evaluated at conditions other than the actual engine environment. In engine development programs and some research programs, initial tests to evaluate heat transfer and aerodynamic performance of turbines are often conducted with actual size prototype hardware at lower gas temperatures and pressures than the actual application. In research programs where many measurements are required along the surface or in the boundary layer to obtain a more

fundamental understanding of a cooling method for turbine blades, large models are used at conditions of essentially ambient temperature and pressure. These practices often raise the question of whether performance at the test conditions will be similar to that under actual engine operation.

Similarity parameters which are important in relating test and engine performance of a cooled turbine blade are defined, the necessary equations developed, and conditions illustrated under which similarity would be obtained. Conditions are derived for a general case of combined film and convection cooling, but the results apply as well to plain convection or plain film cooled hardware. The velocity distribution $u_g/u_{g,cr}$ and momentum thickness Reynolds number $\rho u_g \theta/\mu$ distribution around the turbine blade must be the same between engine and test conditions. Similarity in these two parameters is essential to ensure the same Stanton number distribution and dimensionless adiabatic wall temperature and the same location on the blade for transition from a laminar to a turbulent boundary layer between engine and test conditions.

Let superscript (t) refer to test conditions and superscript (e) refer to engine conditions. To ensure that the local critical Mach number distribution does not change between the two conditions, the equivalent mass flow must be the same in both cases. Therefore,

$$\frac{W_g^{(t)}}{W_g^{(e)}} = \frac{P_g^{(t)}}{P_g^{(e)}} \sqrt{\frac{(RT)_g^{(e)}}{(RT)_g^{(t)}}} \frac{\Gamma_g^{(t)}}{\Gamma_g^{(e)}} \tag{1}$$

where Γ is a correction for the variation of specific heat with temperature given by

$$\Gamma = \sqrt{\gamma}\left(\frac{2}{\gamma+1}\right)^{(\gamma+1)/[2(\gamma-1)]} \tag{2}$$

from reference 3.

Since the local Reynolds number must also remain unchanged between (t) and (e) conditions, the flow rate in equation (1) must vary directly with viscosity; that is,

$$\frac{\left(\frac{\rho u \theta}{\mu}\right)_g^{(t)}}{\left(\frac{\rho u \theta}{\mu}\right)_g^{(e)}} = \frac{\theta_g^{(t)}}{\theta_g^{(e)}} \frac{P_g^{(t)}}{P_g^{(e)}} \frac{\mu_g^{(e)}}{\mu_g^{(t)}} \sqrt{\frac{(RT)_g^{(e)}}{(RT)_g^{(t)}}} \frac{\Gamma_g^{(t)}}{\Gamma_g^{(e)}} = 1 \tag{3}$$

If with film cooling the local film effectiveness is to remain unchanged between engine and test conditions, the coolant- to hot-gas mass flux ratio $(\rho u)_c/(\rho u)_g$, the coolant-to hot-gas momentum ratio $(\rho u^2)_c/(\rho u^2)_g$ (or density ratio ρ_c/ρ_g), and the momentum thickness to film ejection hole diameter ratio θ/d must be the same in both cases. Since actual size hardware is presumed, then

$$\frac{(\theta/d)^{(t)}}{(\theta/d)^{(e)}} = \frac{\theta^{(t)}}{\theta^{(e)}} = 1 \tag{4}$$

and equation (3) becomes

$$\frac{P_g^{(t)}}{P_g^{(e)}} \frac{\mu_g^{(e)}}{\mu_g^{(t)}} \sqrt{\frac{(RT)_g^{(e)}}{(RT)_g^{(t)}}} \frac{\Gamma_g^{(t)}}{\Gamma_g^{(e)}} = 1 \tag{5}$$

Equation (5) gives the functional relation between gas pressure and temperature which will provide the same Reynolds number and critical Mach number distributions for test and engine conditions. Parametric curves of equation (5) are shown in figure 1 for a gas with air properties.

The cooling airflow rate and temperature are then set by the coolant-to-gas mass flux ratio and momentum ratio. Requiring

$$\left[\frac{(\rho u)_c}{(\rho u)_g}\right]^{(t)} = \left[\frac{(\rho u)_c}{(\rho u)_g}\right]^{(e)} \tag{6}$$

implies

$$\left(\frac{W_c}{W_g}\right)^{(t)} = \left(\frac{W_c}{W_g}\right)^{(e)} \tag{7}$$

or

$$\frac{W_c^{(t)}}{W_c^{(e)}} = \frac{W_g^{(t)}}{W_g^{(e)}} = \frac{\mu_g^{(t)}}{\mu_g^{(e)}}$$

Finally, it is necessary that

$$\left(\frac{t_{co}}{t_g}\right)^{(t)} = r\left(\frac{t_{co}}{t_g}\right)^{(e)} \tag{8}$$

to ensure equality of test and engine momentum ratio since $p_{co} = p_g$.

The factor r in equation (8) is a gas constant ratio given by

$$r = \left(\frac{R_{co}}{R_g}\right)^{(e)} \left(\frac{R_g}{R_{co}}\right)^{(t)}$$

where the subscript identifies the gas and refers the temperature at which the gas constant is evaluated. The gas constant ratio r is, in general, not equal to unity. The value is affected by a number of factors such as fuel-air ratio of the combustion gas, gas dissociation at high temperature, and tests conducted with different film injection and mainstream fluids. In many cases, particularly in turbine aerodynamic studies where the effect of film injection on turbine performance is investigated, an injection fluid of lower molecular weight than the mainstream is chosen to reduce the required film temperature $t_{co}^{(t)}$.

Equations (6) and (8) also imply that, at a given film injection location, the coolant-to-gas Mach number ratio at engine and test conditions differs from unity only by the specific heat product

$$\left(\frac{\gamma_g^{(t)}}{\gamma_g^{(e)}}\right) \cdot \left(\frac{\gamma_{co}^{(e)}}{\gamma_{co}^{(t)}}\right)$$

Since this product is usually near unity, similarity in coolant Mach number is also preserved.

Neglecting conduction in the plane of the wall compared to that in the direction normal to the wall, the film ejection temperature T_{co} is related to the supply coolant temperature by

$$\frac{(H_{co} - H_{ci})^{(t)}}{(H_{co} - H_{ci})^{(e)}} = \frac{q^{(t)}}{q^{(e)}} \frac{\mu_g^{(e)}}{\mu_g^{(t)}} \tag{9}$$

where q is the local hot gas-to-vane heat flux.

If the wall temperature is linear as was assumed in the examples of the next section, then the heat flux is given by

$$q = \frac{T_{aw} - T_{ci}}{\frac{1}{h_g} + \frac{1}{h_c} + \frac{L}{k_m}}$$

For a nonlinear wall temperature distribution such as in the case of transpiration cooling through a porous wall, the appropriate expression for heat flux is given in reference 4.

Satisfying equations (5) to (9) ensures that the Stanton number distribution around the blade will be similar for both test and engine conditions. Expressing the heat transfer coefficient in dimensionless Stanton number form gives

$$St_g^{(t)} = St_g^{(e)} \left(\frac{Pr^{(e)}}{Pr^{(t)}} \right)_g^{2/3} \tag{10}$$

Since the Prandtl number cannot be set independently if all other similarity conditions discussed are met, the departure of the Stanton number ratio from unity depends on the Prandtl number ratio in equation (10).

On the coolant side, the heat transfer coefficient in dimensionless Nusselt number form is given by

$$Nu_c^{(t)} = Nu_c^{(e)} \left(\frac{Pr^{(t)}}{Pr^{(e)}} \right)_c^{1/3} \left(\frac{\mu_g^{(t)} \mu_{co}^{(e)}}{\mu_g^{(e)} \mu_g^{(t)}} \right)^n \tag{11}$$

where n is the power on the Reynolds number for coolant side convection. The viscosity factor in equation (11) is the test-to-engine coolant Reynolds number ratio. As with the Prandtl number, this factor cannot be set independently with the existing constraints although its departure from unity is small. In fact, if the viscosity over the full temperature range $t_g^{(e)}$ to $t_{co}^{(t)}$ could be approximated by a power law

$$\mu \propto t^w$$

then by equation (8), the test-to-engine coolant Reynolds number ratio (based on the film cooling hole diameter and the ejection temperature) would be identically one. The same coolant Reynolds number and Mach number between actual and simulated conditions is important to ensure the same percent pressure drop through the internal cooling air passages between the two conditions.

If the cooled blade is to perform the same during a test as it does in the engine, there must be some normalized outer wall temperatures which remains invariant between test and engine conditions. The most convenient dimensionless wall temperature includes only those temperatures which are a priori known, namely the coolant supply temperature T_{ci} and the effective gas temperature T_{ge}. Hence, the dimensionless wall temperature φ, defined as

$$\varphi = \frac{T_{ge} - T_{wo}}{T_{ge} - T_{ci}} \tag{12}$$

or some similar grouping of these three temperatures is commonly used as a measure of the cooling performance of a given blade design.

Strict equality in φ test-to-engine is impossible with actual hardware because the temperature drop through the wall is not scaled properly over a wide range of test conditions with temperature variable wall thermal conductivity. However, for properly scaled test conditions, the difference between $\varphi^{(t)}$ and $\varphi^{(e)}$ is well within the range of experimental accuracy in most cases.

In summary, when the engine condition is completely specified (including external and internal heat transfer coefficients, film effectiveness, percent coolant flow, etc.), equations (5) and (7) to (11) are solved simultaneously for the test variables $P_g^{(t)}$, $T_g^{(t)}$, $T_{ci}^{(t)}$, $W_g^{(t)}$, and $W_c^{(t)}$ which satisfy the similarity constraints discussed in this section. With these six equations, there is still one degree of freedom, but once any one of the five variables is specified, the remaining four are fixed.

APPLICATION OF SIMILARITY PARAMETERS TO ENGINE AND TEST ENVIRONMENTS

Test Constraints

The similarity parameters and constraints presented in the preceding section are applied to engine conditions summarized in table I to illustrate a range of test conditions which preserve similarity. Examples are also shown for test conditions which do not

satisfy similarity constraints to illustrate the errors that are encountered when test conditions are chosen improperly.

The test turbine inlet gas temperature and pressure is a function of the supplying cooling air temperature. The lower this cooling air temperature is, the lower the gas temperature and pressure must be to simulate a given engine condition. If ambient temperature air is used for cooling, the various engine conditions in table I can be simulated in a moderate test environment of pressures ranging from 1.5 to 10.5 atmospheres and temperatures ranging from 578 to 878 K (580° to 1120° F). Figure 2 maps all of the engine conditions of table I on a turbine inlet pressure and temperature field by tailed symbols. The corresponding simulation test condition for ambient cooling air is indicated on the figure by the same symbol untailed. In all 16 takeoff and cruise test simulations indicated in the figure, only in the case of the 2478 K (4000° F) gas temperature advanced technology transport did $\varphi^{(t)}$ exceed $\varphi^{(e)}$ by more than 1 percent (and that was by 1.9 percent).

Representative examples of other similarity-preserving test gas environments are illustrated in table II for cooling air temperatures other than ambient. The tables show the engine (or reference) environments and possible test environments for both the engine cruise and takeoff conditions. The entries corresponding to a 294 K (70° F) cooling air temperature are common with figure 2. Test facilities are often limited in gas pressure or temperature or both. Table II illustrates how similarity constraints coupled with facility limitations can impose an upper limit on the coolant supply temperature. Conversely, since it is usually undesirable to cool the cooling air below ambient temperature, a lower limit on gas temperature and pressure is imposed. Consequently, for many existing test rigs there is only a narrow pressure-temperature test range of practical interest. Consider, for example, the ATT engine in table II(b) under takeoff conditions. In this case, the lowest test gas pressure that can simulate the engine condition without cooling the cooling air below 294 K (70° F) is 10.3 atmospheres. Many test facilities cannot operate at pressures even this high. Also included in table II is the test-to-engine dimensionless wall temperature φ. As pointed out in the preceding section, this temperature ratio is greater than one because similarity in conduction through the blade wall with temperature variable thermal conductivity is not achieved over the wide range of test conditions shown in the table. However, in the usual case where the metal thermal conductivity increases with temperature, nonsimilar conduction effects are often of secondary importance. This is definitely true of the examples in table II in which the blade thermal conductivity corresponded to MAR-M alloy 509 material. The difference between $\varphi^{(t)}$ and $\varphi^{(e)}$ in the table is well within acceptable limits of experimental accuracy.

It can be concluded from these results of dimensionless wall temperature that, if testing is done at the proper reduced gas temperature and pressure, the cooled blade

will behave similarly in the test as it does during actual engine operation. However, care must be exercised in interpreting test results as directly representing performance under engine conditions. All the factors contributing to the net heat flux to the test surface must be accounted for in both the test and engine environments. For instance, radiation can be a significant component of the total heat flux to a blade or combustor liner under high temperature and pressure conditions. Since radiation cannot be conveniently simulated at a low temperature and pressure test condition, it should be accounted for in the heat flux ratio $q^{(t)}/q^{(e)}$ in equation (9). Another factor to consider is that frequently combustion air (or unvitiated hot gas) in test facilities picks up rust or other oxides from the interior walls of the supply piping and deposits it on the test surface. This layer of rust can act as an insulating buffer layer or change the surface emissivity or even change the location on the surface of transition from a laminar to a turbulent boundary layer. The first two effects can be accounted for in the heat flux ratio if such deposits are a problem. The latter effect, that of altering the location of boundary layer transition would change the test-to-engine similitude conditions based on testing actual engine hardware. Still another factor which affects boundary layer development and the convective heat flux, especially in a highly accelerated flows such as over a turbine blade, is the free stream turbulence. It is unlikely that the turbulent structure would be scaled properly between test and engine conditions. Surface roughness and free stream turbulence effects could probably best be accounted for by analytically adjusting the dimensionless wall temperature test results. This would require solving the boundary layer equations with free stream turbulence and surface roughness as specified boundary conditions. This is assuming, of course, that the turbulent structure in the engine was known.

Boundary Layer Similarity

The triad of state properties (P_g, T_g, and T_{ci}) in equations (5) to (9) were determined using properties based on inlet static conditions. In reality, properties vary continuously through the boundary layer and along the surface. Equations (5) to (11) could be adjusted by a surface-to-gas temperature ratio factor to account for this property variation, but in most cases, it is not necessary. To verify the similarity relations using properties evaluated at the static inlet temperature, the boundary layer development around the suction side of a turbine blade was investigated analytically for engine and test conditions. A finite difference boundary layer program conserving momentum, energy, and turbulent kinetic energy was solved using a modified Spalding-Patanker (ref. 5) numerical procedure. Properties are evaluated locally through the boundary layer at each grid point. The results are shown in figure 3 for the 2200 K (3500° F)

turbine inlet temperature CTOL (ATT) engine of table I at takeoff conditions. Curves of momentum thickness θ, momentum thickness Reynolds number Re_θ, and Stanton number St as a function of dimensionless distance from the blade leading edge on the suction side are given for the engine condition. Corresponding test condition results are shown in terms of the percent deviation from these values. The test condition chosen for this illustration is that corresponding to unheated 294 K (70° F) cooling air (see table II(b) and fig. 2). The similarity relations indicate that the surface temperature of the blade, which is 1311 K (1900° F) in the engine, will be 451 K (352° F) in the test simulation. This surface temperature is used as a boundary condition in the numerical procedure. The results shown illustrate that the engine boundary layer momentum and heat transfer behavior is duplicated very closely at the reduced temperature and pressure of the test condition. In fact, the test-to-engine Stanton number ratio is closer to unity than would be expected from equation (10). Transition from a laminar boundary layer occurs at essentially the same location for both the engine and the test - at approximately 12 percent of the suction surface length from the leading edge.

Errors Resulting From an Indiscriminate Selection of Test Conditions

To illustrate the errors encountered when test conditions do not preserve similarity with the engine environment, suppose hardware from the 2200 K (3500° F) turbine inlet temperature, ATT engine is tested at gas pressures of 1, 2, and 6 atmospheres and at a temperature the same as that of the engine. Recall that the combustor exit pressure of the engine is 33.7 atmospheres at takeoff conditions. Frequently, testing is done at such nonsimilar conditions simply to demonstrate cooling performance at high temperatures, but as we will see, the results can be very misleading. Distributions of momentum thickness Reynolds number and Stanton number along the suction side of the turbine blade considered in the previous section were determined for each of the three example test conditions. The results are shown in figure 4. The figure clearly shows the departure of the heat transfer and boundary layer behavior between the test and the engine when the pressure and temperature do not satisfy equation (5). The performance of a complex blade design, particularly one incorporating a combination of film and convection cooling cannot be properly evaluated if testing is done at such nonsimilar "off-design" conditions. Local high heat flux regions of the blade would shift to different locations under test conditions resulting in a misleading indication of surface temperature distribution. Also, the transition from a laminar to a turbulent boundary layer would occur at a blade surface location different from that of the engine. As the pressure is reduced, boundary layer transition is delayed further back from the leading edge. At pressures of 1 and 2 atmospheres, the boundary layer never becomes turbulent. The trailing edge momentum thickness Reynolds number for the engine exceeds 6000 but

never gets larger than 250 for the test pressures of 1 and 2 atmospheres.

Consider, for example, the 30 percent location on the blade where the boundary layer is fully turbulent in the engine environment and compare it with the 1 atmosphere test condition which is still laminar at that location. One would conclude from the test results that the wall temperature would run 243 K (438° F) cooler at this location than it actually does under engine conditions, or in terms of dimensionless wall temperature, $\varphi^{(e)}$ is 0.56 and $\varphi^{(t)}$ is 0.74. Of course, this is an extreme example, but it does illustrate how one could falsely be led to believe, based on low pressure tests, that the blade could easily be cooled.

It is obvious from figure 4 that care must be exercised in setting test conditions if meaningful results are to be obtained. It is not sufficient to simply provide a high heat flux by raising the gas temperature to demonstrate cooling performance while ignoring the pressure level.

Effect of Test Hardware Scale

Most of the discussion has been based on the assumption that actual size hardware is to be tested in a development-type program. If testing on a more basic level is required, a larger scale model may be necessary. In this case, test pressure and temperature constraints can be relaxed. The similarity equations still apply, but since the test momentum thickness $\theta^{(t)}$ is greater than the engine momentum thickness $\theta^{(e)}$ by the size scale factor (see eq. (4)), the factor $(P/\sqrt{T})_g^{(t)}$ can be reduced by the value of the scale factor and gas properties as seen from equation (3). For this reason, the large scale test hardware or models can be investigated at near ambient temperature and atmospheric pressure and still simulate (except for Mach number) an actual engine environment. The low pressure, and particularly the low temperature, greatly reduces the cost and complexity of the facility, test models, and instrumentation as well as providing conditions favorable for detailed boundary layer and heat transfer measurements.

CONCLUDING REMARKS

Analysis indicates that low gas pressure and temperature test environments can simulate basic engine heat transfer and aerodynamic performance of turbine hardware expected in current and future gas turbine engines. Testing at low gas temperatures and pressures can reduce the cost and complexity of test facilities, models, and instrumentation and also provide conditions favorable for detailed measurements. Once any one of the test variables among hot gas pressure, temperature, and flow rate, and cool-

ing air supply temperature and flow rate is selected, the remaining four are fixed by similarity constraints.

Frequently, the objective of heat transfer tests is simply to demonstrate cooling performance at high temperature without regard to pressure level. Such tests can be very misleading. Departure from strict adherence to similarity constraints because of test facility limitations or other reasons, can result in a number of serious errors in projecting the performance of test hardware to engine conditions.

Lewis Research Center,
National Aeronautics and Space Administration,
Cleveland, Ohio, April 3, 1974,
501-24.

REFERENCES

1. Thomas, B. K., Jr.: New Wing Promises Design Breakthrough. Aviation Week and Space Tech., vol. 87, no. 4, July 24, 1967, pp. 25-26.
2. Dugan, James F., Jr.: Engine Selection for Transport and Combat Aircraft. NASA TM X-68009, 1972.
3. Glassman, Arthur J., ed.: Turbine Design and Application, Volume 1. NASA SP-290, 1972.
4. Colladay, Raymond S.; and Stepka, Francis S.: Examination of Boundary Conditions for Heat Transfer Through a Porous Wall. NASA TN D-6405, 1971.
5. Patankar, S. V.; and Spalding, D. B.: Heat and Mass Transfer in Boundary Layers. C.R.C. Press, 1967.

TABLE I. - COMBUSTION GAS ENVIRONMENTS OF ADVANCED AIRCRAFT ENGINES

Airplane type	Takeoff							Cruise								
	Combustor exit			Overall pressure ratio	Bypass pressure ratio	Cooling air temperature		Combustor exit			Overall pressure ratio	Flight Mach number	Altitude		Cooling air temperature	
	Temperature		Pressure, std atm					Temperature		Pressure, std atm			km	ft		
	K	°F				K	°F	K	°F						K	°F
CTOL (ATT)	1533	2300	24.5	25.0	5.9	772	930	1533	2300	10.1	30.0	0.98	12.19	40 000	730	855
	1728	2650	25.9	26.4	7.8	784	952	1728	2650	10.7	32.0	.98	12.19	40 000	744	880
	2200	3500	33.7	34.4	8.1	848	1066	2200	3500	13.8	41.2	.98	12.19	40 000	802	983
	2478	4000	36.0	36.8	9.6	865	1097	2478	4000	14.8	44.0	.98	12.19	40 000	817	1011
Integral VTOL	1589	2400	11.9	12.0	11.5	621	658	1589	2400	8.6	13.0	0.75	6.1	20 000	608	635
Remote VTOL	1478	2200	14.25	15.0	1.4	664	735	1478	2200	8.5	16.0	.75	7.62	25 000	621	658
STOL	1505	2250	15.7	16.0	14.9	677	758	1505	2250	8.8	16.3	0.75	7.62	25 000	624	664
SST	1769	2725	9.6	10.0	2.0	589	600	1769	2725	4.7	4.0	2.7	19.8	65 000	810	998

TABLE II. - SIMILARITY STATES

(a) Low temperature CTOL (ATT) aircraft

Turbine inlet temperature		Turbine inlet pressure, atm	Coolant temperature		W_g ratio (test-to-engine)	φ ratio (test-to-engine)
K	^{o}F		K	^{o}F		
Takeoff						
[a]1533	[a]2300	[a]24.5	[a]772	[a]930	----	----
367	200	4.7	189	-119	0.40	1.02
478	400	6.5	244	-21	.48	1.01
582	587	8.2	294	70	.55	1.00
589	600	8.3	298	76	.56	
700	800	10.2	352	173	.63	
811	1000	12.1	406	271	.69	
922	1200	14.0	460	368	.74	
1033	1400	15.9	516	469	.80	
1144	1600	17.8	573	571	.85	
1255	1800	19.7	630	674	.89	
1367	2000	21.6	687	777	.94	
1478	2200	23.5	744	880	.98	
Cruise						
[a]1533	[a]2300	[a]10.1	[a]730	[a]855	----	----
367	200	1.9	181	-134	0.40	1.02
478	400	2.7	232	-42	.48	1.01
584	600	3.4	283	49	.56	1.01
614	646	3.6	294	70	.58	1.01
700	800	4.2	333	139	.63	1.00
811	1000	5.0	384	231	.69	
922	1200	5.8	434	322	.74	
1033	1400	6.5	488	418	.80	
1144	1600	7.3	541	514	.85	
1255	1800	8.1	595	612	.89	
1367	2000	8.9	649	709	.94	
1478	2200	9.7	704	808	.98	

[a]Engine condition; all other values are similarity states.
states.

TABLE II. - Continued. SIMILARITY STATES

(b) High temperature CTOL (ATT) aircraft

Turbine inlet temperature		Turbine inlet pressure, atm	Coolant temperature		W_g ratio (test-to-engine)	φ ratio (test-to-engine)
K	^{o}F		K	^{o}F		
Takeoff						
$^{a}2200$	$^{a}3500$	$^{a}33.7$	$^{a}848$	$^{a}1066$	----	----
367	200	4.3	145	-199	0.33	1.04
478	400	6.0	188	-122	.39	1.03
589	600	7.7	230	-45	.46	1.02
700	800	9.4	273	31	.51	1.01
758	905	10.3	294	70	.54	1.01
811	1000	11.1	315	107	.56	1.01
922	1200	12.9	357	182	.60	1.00
1033	1400	14.6	399	259	.65	
1144	1600	16.4	442	335	.69	
1255	1800	18.2	485	413	.73	
1367	2000	19.9	528	490	.76	
1478	2200	21.7	571	568	.80	
1589	2400	23.5	613	644	.83	
1700	2600	25.3	656	721	.86	
1811	2800	27.1	699	799	.89	
1922	3000	28.9	743	878	.92	
2033	3200	30.9	786	955	.96	
2144	3400	32.8	828	1030	.99	
Cruise						
$^{a}2200$	$^{a}3500$	$^{a}13.8$	$^{a}802$	$^{a}983$	----	----
367	200	1.8	139	-209	0.33	1.03
478	400	2.5	180	-136	.39	1.02
589	600	3.2	220	-64	.46	1.01
700	800	3.9	259	7	.51	1.01
799	978	4.5	294	70	.55	1.01
811	1000	4.6	299	78	.56	1.01
922	1200	5.3	338	148	.60	1.00
1033	1400	6.0	378	220	.65	
1144	1600	6.7	417	291	.69	
1255	1800	7.4	458	364	.73	
1367	2000	8.2	498	437	.76	
1478	2200	8.9	539	510	.80	
1589	2400	9.6	579	582	.83	
1700	2600	10.4	619	655	.86	
1811	2800	11.1	660	729	.89	
1922	3000	11.8	702	804	.92	
2033	3200	12.7	743	878	.96	
2144	3400	13.4	782	948	.99	

[a]Engine condition; all other values are similarity states.

TABLE II. - Continued. SIMILARITY STATES

(c) Integral VTOL aircraft

Turbine inlet temperature		Turbine inlet pressure, atm	Coolant temperature		W_g ratio (test-to-engine)	φ ratio (test-to-engine)
K	^{o}F		K	^{o}F		
Takeoff						
[a]1589	[a]2400	[a]11.9	[a]621	[a]658	----	----
367	200	2.2	153	-185	0.39	1.03
478	400	3.0	195	-109	.46	1.02
589	600	3.9	236	-35	.55	1.01
700	800	4.8	277	38	.61	1.01
748	886	5.1	294	70	.64	1.01
811	1000	5.6	318	112	.67	1.00
922	1200	6.5	359	186	.73	↓
1033	1400	7.4	395	262	.78	
1144	1600	8.3	443	337	.83	
1255	1800	9.2	488	419	.87	
1367	2000	10.1	532	498	.92	
1478	2200	11.0	577	578	.96	↓
Cruise						
[a]1589	[a]2400	[a]8.6	[a]608	[a]635	----	----
367	200	1.6	150	-190	0.39	1.03
478	400	2.1	191	-116	.46	1.02
589	600	2.8	231	-44	.55	1.02
700	800	3.4	271	28	.61	1.01
765	918	3.8	294	70	.65	1.01
811	1000	4.1	311	100	.67	1.00
922	1200	4.7	352	173	.73	↓
1033	1400	5.4	393	247	.78	
1144	1600	6.0	433	320	.83	
1255	1800	6.7	477	399	.87	
1367	2000	7.3	521	478	.92	
1478	2200	7.9	564	556	.96	↓

[a]Engine condition; all other values are similarity states.

TABLE II. - Concluded. SIMILARITY STATES

(d) SST aircraft

Turbine inlet temperature		Turbine inlet pressure, atm	Coolant temperature		W_g ratio (test-to-engine)	φ ratio (test-to-engine)
K	^{o}F		K	^{o}F		
Takeoff						
[a]1769	[a]2725	[a]9.6	[a]588	[a]599	----	----
367	200	1.6	132	-223	0.37	1.04
478	400	2.2	169	-156	.45	1.03
589	600	2.8	204	-92	.52	1.02
700	800	3.4	239	-30	.58	1.01
811	1000	4.1	273	32	.63	1.01
877	1118	4.4	294	70	.66	1.01
922	1200	4.7	308	95	.69	1.00
1033	1400	5.3	344	159	.73	
1144	1600	6.0	379	223	.78	
1255	1800	6.6	415	288	.82	
1367	2000	7.3	452	353	.86	
1478	2200	7.9	490	423	.90	
1589	2400	8.6	527	488	.94	
1700	2600	9.2	564	556	.97	
Cruise						
[a]1769	[a]2725	[a]4.7	[a]810	[a]998	----	----
367	200	.8	173	-149	0.37	1.02
478	400	1.1	223	-59	.45	1.01
589	600	1.4	272	30	.52	1.01
639	691	1.5	294	70	.54	1.01
700	800	1.7	321	118	.58	1.00
811	1000	2.0	370	206	.63	
922	1200	2.3	420	296	.69	
1033	1400	2.6	470	386	.73	
1144	1600	2.9	521	478	.78	
1255	1800	3.2	572	570	.82	
1367	2000	3.6	624	663	.86	
1478	2200	3.9	675	756	.90	
1589	2400	4.2	726	847	.94	
1700	2600	4.5	778	940	.97	

[a]Engine condition; all other values are similarity states.

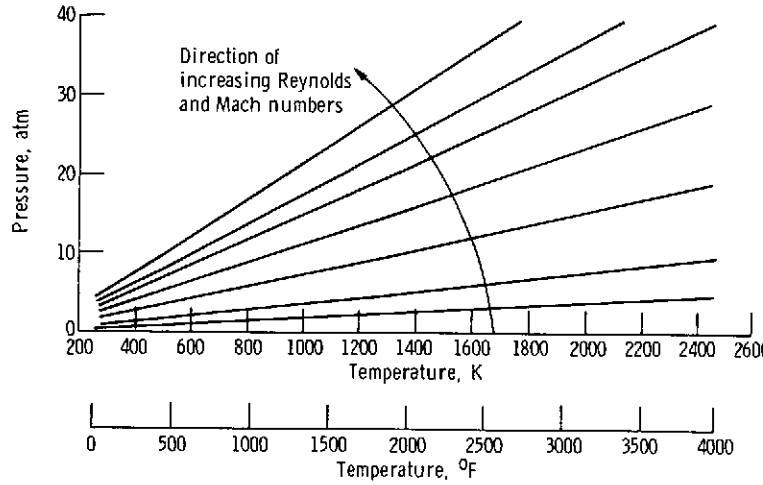

Figure 1. - Similarity curves of constant critical Mach number and momentum thickness Reynolds number distributions around turbine vane.

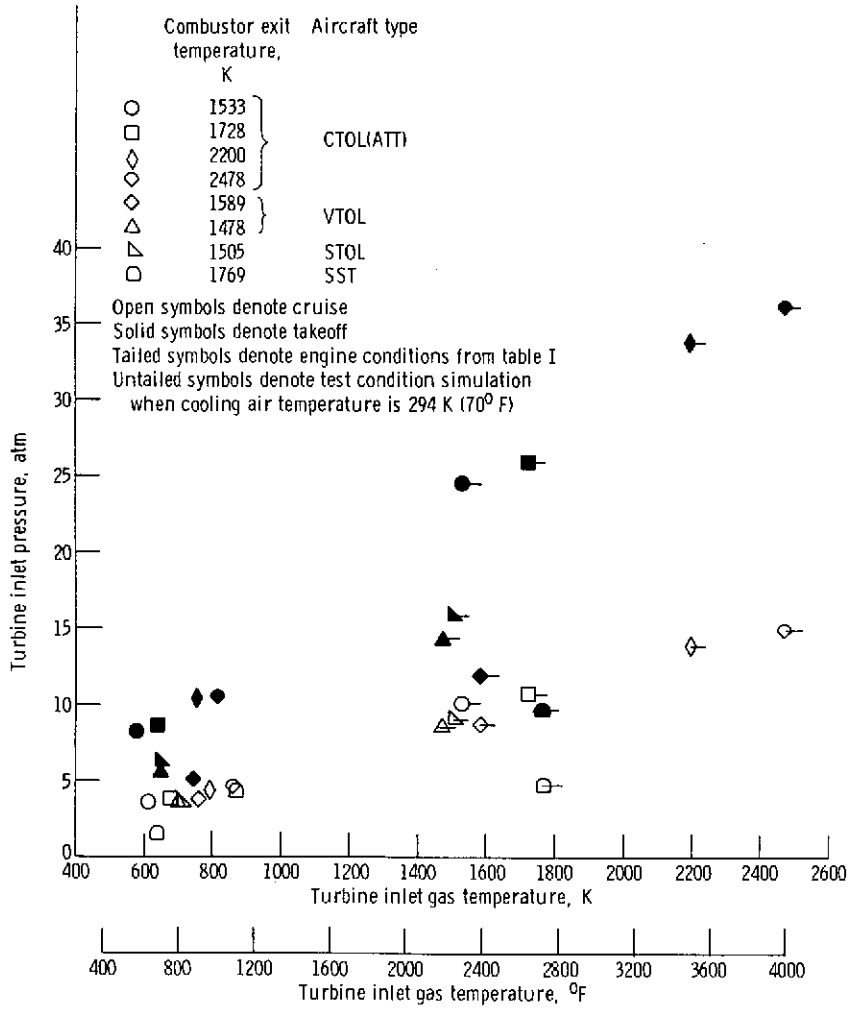

Figure 2. - Simulated test conditions for unheated cooling air.

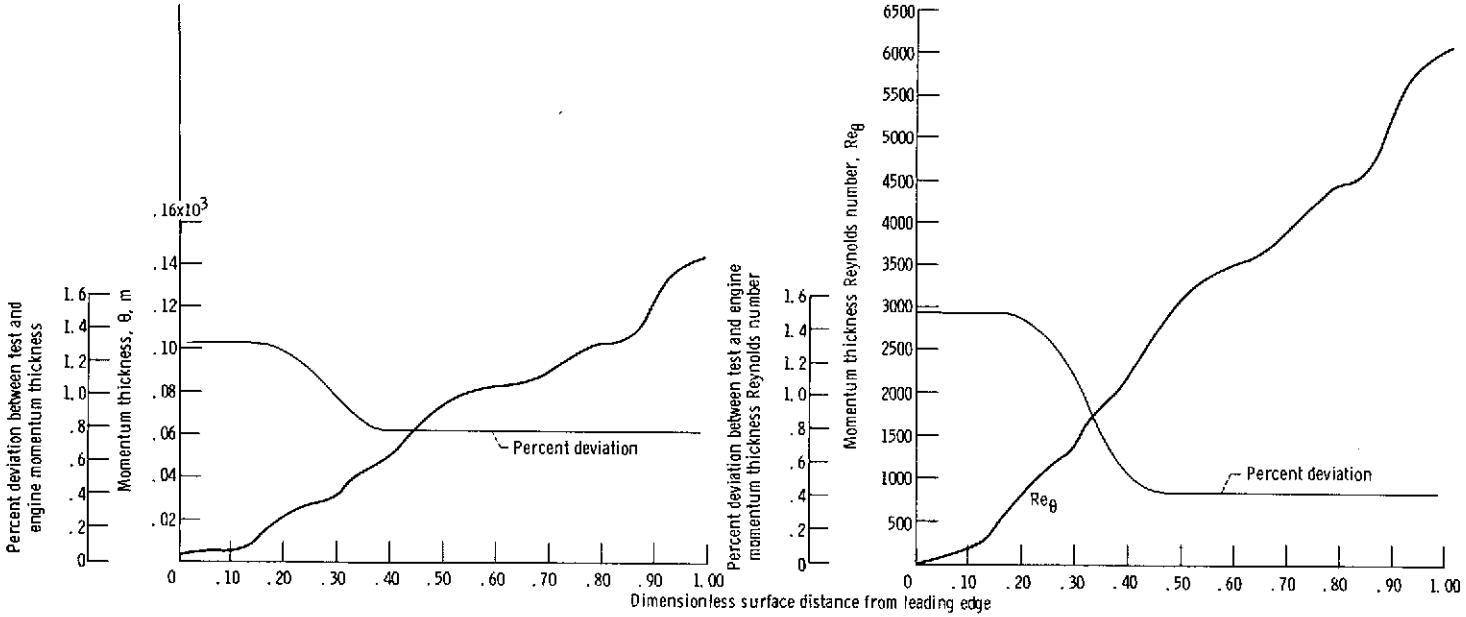

(a) Momentum thickness distribution.

(b) Boundary layer momentum thickness Reynolds number distribution.

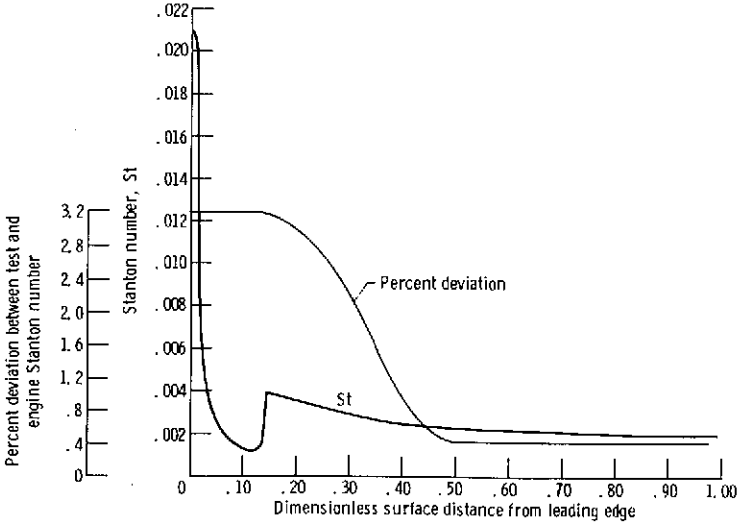

(c) Stanton number distribution.

Figure 3. - Boundary layer momentum and heat transfer distributions around suction side of high bypass core turbine blade for 2200 K (3500° F) turbine inlet temperature ATT engine condition (turbine inlet pressure of 33.7 atm at takeoff) and deviation of similarity preserving test condition ($T_g^{(t)}$ = 758 K (905° F) and $P_g^{(t)}$ = 10.3 atm) from engine condition.

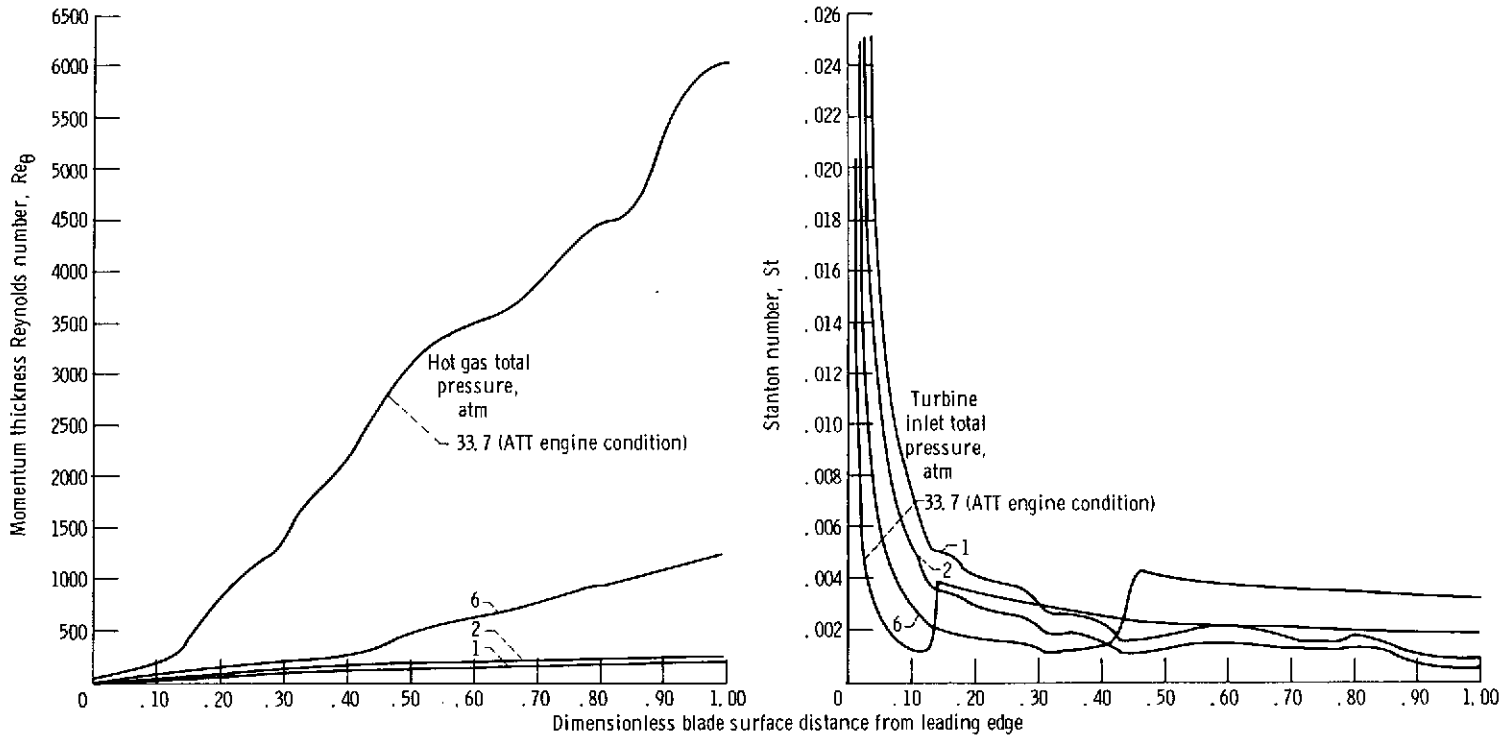

(a) Boundary layer momentum thickness Reynolds number.

(b) Stanton number distribution.

Figure 4. - Effect of pressure on similarity of momentum and heat transfer distribution for suction side of high bypass core turbine blade. Gas temperature T_{ge} = 2200 K (3500° F).